Journal of Hydrology 606 (2022) 127400

Contents lists available at ScienceDirect

Journal of Hydrology

journal homepage: www.elsevier.com/locate/jhydrol

Research papers

Changes in rain and snow over the Tibetan Plateau based on IMERG and Ground-based observation

Donghuan Li [a,b], Youcun Qi [a,b,*], Deliang Chen [c]

[a] Key Laboratory of Water Cycle and Related Land Surface Processes, Institute of Geographic Sciences and Natural Resources Research, Chinese Academy of Sciences, Beijing, China
[b] University of Chinese Academy of Sciences, Beijing, China
[c] Regional Climate Group, Department of Earth Sciences, University of Gothenburg, Gothenburg, Sweden

ARTICLE INFO

Keywords:
IMERG
Ground-based observation
Rain
Snow
Tibetan Plateau

ABSTRACT

The latest generation of satellite precipitation estimates, Integrated Multi-satellitE Retrievals for Global Precipitation Measurement Version 06 (IMERG V06), calibrated by monthly rain gauge data, is applied to investigate the changing characteristics of precipitation in different phases (rain, snow, and sleet) over the Tibetan Plateau (TP) from 2001 to 2020. The performance of the IMERG product in capturing the characteristics of the three precipitation phases is firstly evaluated against the ground-based observation. The results show that the IMERG product performs well in capturing the spatial distribution, magnitudes, and annual cycle of the amount and frequency of precipitation in different phases. The bias of annual precipitation amount (frequency) averaged in the 90 stations used in this study is approximately 10% (20%). Comparatively, the IMERG product shows higher skill in estimating rain than snow, and performs better in the other three seasons than in winter. In addition, the performance of the IMERG product is comparable in the southern and northern TP. Both the annual amount and frequency of precipitation have increased in most parts of the TP in the last two decades, with maximal values of 50 mm and 20 days per decade, respectively, occurring in the central part of eastern TP. Changes in the amount and frequency of precipitation are dominated by rain and snow, respectively, in the study period. In addition, light and moderate precipitation contribute approximately 70% and 90% to the increases of the regional mean precipitation amount and frequency, respectively, in the central part of eastern TP. There are no significant and uniform changes in the snowy season during the last two decades, therefore, the increase in snowy days in most areas of the TP is caused by more frequent snow events in the fairly constant snowy season.

1. Introduction

The Tibetan Plateau (TP) is the highest plateau in the world with an average elevation of over 4000 m a.s.l., exerting a very important influence on the climate in Asia and beyond (Duan and Wu, 2005; Wu et al., 2012; Yao et al., 2012). Known as the "Asian water tower", the TP and the adjacent mountain ranges are the sources of all the major rivers in Asia, and play an important role in the climate, water resources and ecosystem of the downstream regions (Immerzeel et al., 2010; Immerzeel and Bierkens, 2012). Precipitation is one of the most important and active components of the water cycle and has been changed under global warming in the past several decades (IPCC, 2013).

The TP has experienced evident climate change since the 1960 s, including the overall warming, glacier shrinking, and water cycle changing (Yao et al., 2007; Kang et al., 2010; Yang et al., 2014). The changes of precipitation over the TP in the past several decades are spatially different and exhibit evident decadal variability (Xu et al., 2007). The regional mean annual precipitation over the TP showed fluctuating increase in the last decades. For the periods of 1961–2012, 1971–2005, and 1971–2011, the increasing rates of annual precipitation averaged over the TP are 5 mm, 12 mm, and 7.5 mm per decade, respectively (Wu et al., 2007; Gao et al., 2014; Kuang and Jiao, 2016; Wang et al., 2018). The precipitation increased in central and eastern and decreased in western parts of the TP during 1961–2001 (Xu et al., 2008). The annual precipitation averaged over southeastern and northwestern TP increased by 16.8 mm and 4 mm per decade from 1979

* Corresponding author at: Key Laboratory of Water Cycle and Related Land Surface Processes, Institute of Geographic Sciences and Natural Resources Research, Chinese Academy of Sciences, Beijing, China.
E-mail address: Youcun.Qi@igsnrr.ac.cn (Y. Qi).

https://doi.org/10.1016/j.jhydrol.2021.127400
Received 13 July 2021; Received in revised form 20 November 2021; Accepted 23 December 2021
Available online 30 December 2021

to 2001, respectively (You et al., 2015). Changes in precipitation over the TP also show seasonal features. Winter precipitation increased slightly in most parts of the TP from 1961 to 2012, while summer precipitation also increased in most parts of the TP but decreased insignificantly over southeastern TP (Wang et al., 2018). Spring and winter precipitation significantly increased in central and eastern parts of the TP from 1961 to 2007 (You et al., 2012). Precipitation in May increased significantly by 13.36% per decade over southeastern TP during 1979–2014 (Zhang et al., 2017).

Most existing studies on precipitation over the TP do not explicitly treat precipitation in different forms, although solid (snow) and liquid (rain) precipitation have different effects on the water cycle and energy balance (Marks and Dozier, 1992; Loth et al., 1993; Slater et al., 2001; Clark et al., 2006; Dai, 2008). Climate change will influence snowfall and further influence the snowmelt and snow cover (Barnett et al., 2005; Huang et al., 2017). Ground-based observation is the most direct method to obtain precipitation phases. However, it is often insufficient or not accessible. Therefore, many previous studies classified precipitation phases based on surface air temperature, wet-bulb temperature, and other atmospheric conditions (Auer, 1974; Clark et al., 2006; Ding et al., 2014).

Based on the temperature threshold, the regional mean snowfall and snowfall/rainfall ratio decreased by 6 mm and 5% per decade over the TP from 1961 to 2013 (Wang et al., 2016). Based on the classification method proposed by Ding et al. (2014), The snowfall trends during 1960–2014 show large spatial variation, increasing in central and western and decreasing in eastern and northeastern TP (Deng et al., 2017). Based on temperature and relative humidity thresholds, snowfall increased in eastern TP and decreased in western TP during 1961–2007 in the APHRO dataset (Bai et al., 2019). There are uncertainties in estimated snowfall changes over the TP in observational studies, and these can stem from different datasets used, different classification methods, and complex climate regimes over the TP.

Ground-based observation is the most common tool to observe precipitation, and the results above are mainly based on station data or the gridded datasets interpolated from station data. However, rain gauges are sparsely distributed over the TP (Tong et al., 2014b), and the spatial scale of precipitation over the TP is overall small (Chen et al., 2016). Satellite-based precipitation products are of great value to precipitation estimates over mountainous regions, owing to their fine spatial and temporal resolution (Tong et al., 2014a). The Tropical Rainfall Measuring Mission (TRMM) was launched in 1997 (Kummerow et al., 1998), and many satellite-based precipitation retrieval algorithms have been generated based on the multiple satellite sensors, such as Global Satellite Mapping of Precipitation (GSMaP, Kubota et al., 2007), Climate Prediction Center morphing method (CMORPH, Joyce et al., 2004), and TRMM Multi-satellite Precipitation Analysis (TMPA, Huffman et al., 2007).

To further improve the capacity and accuracy of global precipitation observation, the Global Precipitation Measurement (GPM) mission was launched in 2014 (Hou et al., 2014) by the National Aeronautics and Space Administration (NASA) and the Japan Aerospace Exploration Agency (JAXA). The GPM mission is an international network of satellites that provide global observations of rain and snow. The Integrated Multi-satellitE Retrievals for GPM (IMERG, Huffman et al., 2019) algorithm combines information from whatever constellation of satellites operating around Earth at a given time to estimate precipitation over the majority of the Earth's surface. In other words, the IMERG algorithm uses the precipitation estimates collected in both the TRMM and GPM eras to obtain a set of global precipitation records as long as possible.

Previous studies show that the IMERG product exhibits overall good performance in estimating precipitation in different regions around the world by comparing with the ground-based observation (Pradhan et al., 2022). The IMERG product performs well in rainfall detection over the United Arab Emirates from 2010 to 2018, especially the moderate and intense rainfall (Alsumaiti et al., 2020). It shows the potential to complement ground-based observations over Canada (Moazami and Najafi, 2021) and agrees well with gauge-based precipitation over mainland China, Australia and Europe (Navarro et al., 2019; Jiang and Bauer-Gottwein, 2019; Islam et al., 2020). In addition, the IMERG product can accurately capture the general pattern of tropical cyclone precipitation and provides a noticeable improvement in accuracy over its predecessor, TMPA (Yuan et al., 2021). However, there are still biases in the IMERG, such as vacancy report of precipitation occurrence, overestimation of light precipitation and underestimation of heavy precipitation (Navarro et al., 2019; Alsumaiti et al., 2020; Moazami and Najafi, 2021; Yuan et al., 2021).

Tang et al. (2020) compared the performance of the IMERG product with nine satellite and reanalysis precipitation products in China from 2000 to 2018 and indicate that IMERG performs well at the daily and hourly scale. They also investigated the snowfall product in the IMERG product but did not evaluate it against observed rain and snow records on the ground. It is worth noting that the snowfall retrieval algorithm in the IMERG product depends on wet-bulb temperature and needs to be evaluated before applying it in the investigation of snowfall changes.

In this study, we first use the precipitation phase information (rain, snow, and sleet) obtained from the weather station observation network of China to evaluate whether the IMERG product could be used to investigate the precipitation in different phases over the TP. Then changes of precipitation over the TP in different phases during the recent two decades are investigated. We aim to address the following three questions: (1) Weather the IMERG product can reasonably capture the characteristics of rain, snow, and sleet over the TP? (2) How did precipitation in different phases change in the recent two decades? (3) What are the seasonal characteristics of precipitation changes and how precipitation in different intensity levels contribute to the total precipitation changes?

The rest of this paper is organized as follows: Section 2 describes the data and methods used. The main results are exhibited in section 3. The summary and conclusions are given in section 4.

2. Data and methods

2.1. IMERG product

The IMERG final run product (Huffman et al., 2019) is used in this study. The latest version of IMERG product currently is version 06 (V06), containing a comprehensive estimate of rain and snow since June of 2000. The time resolution is 30 min and the spatial resolution is 0.1°. Two variables are used to investigate the characteristics of precipitation in different phases over the TP, the first one is precipitation calibrated at a monthly scale based on gauge analysis and the other one is the probability of liquid precipitation (PL). PL is calculated based on wet-bulb temperature using the method raised by Sims and Liu (2015). Since this diagnostic is independent of the estimated precipitation, the PL is reported for all grid boxes, including those with missing or zero estimated precipitation. In another word, this variable can be applied to other global precipitation fields for estimating precipitation phase.

2.2. Rain gauge data from meteorological stations

The 3-hourly rain, snow, and sleet record, and daily precipitation amount from 90 national ground stations over the TP (circles in Fig. 2a) during 2010–2013 are used. The precipitation amount has undergone strict quality control by China Meteorological Administration (CMA), including climatic range check, internal consistency check, spatiotemporal consistency check, and man-computer interaction control (Ren et al., 2015). The precipitation phases are recorded based on the visual observation of professional weather recorders.

The precipitation-phase data is derived from the Meteorological Information Comprehensive Analysis and Processing System (MICAPS, Li et al., 2010) and quality-controlled according to the following

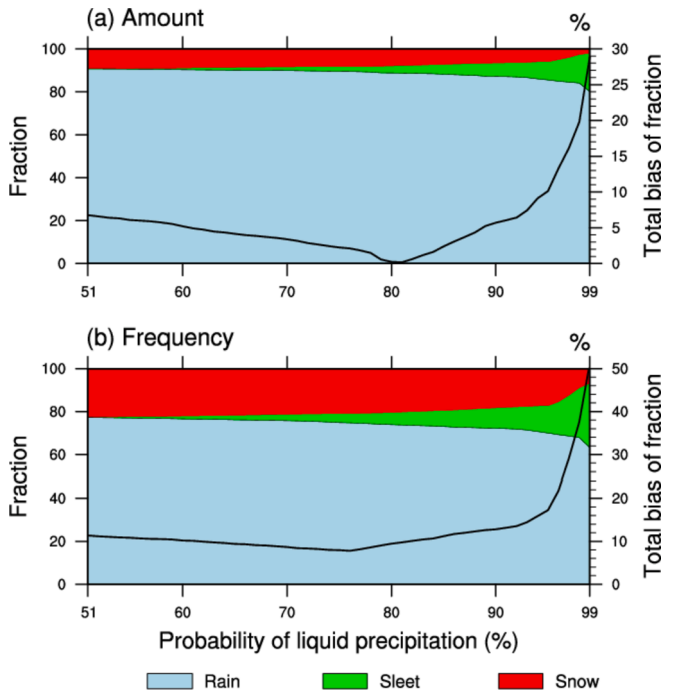

Fig. 1. Determination of the threshold of liquid precipitation probability to distinguish rain, sleet, and snow over the TP. The left Y-axis represents the fractions of (a) amount and (b) frequency of precipitation in different phases, and the right Y-axis represents the total absolute biases of precipitation in different phases. Different colors represent different precipitation phases and the solid line is the sum of the absolute biases of the proportions of rain, snow and sleet with values shown in the right Y-axis.

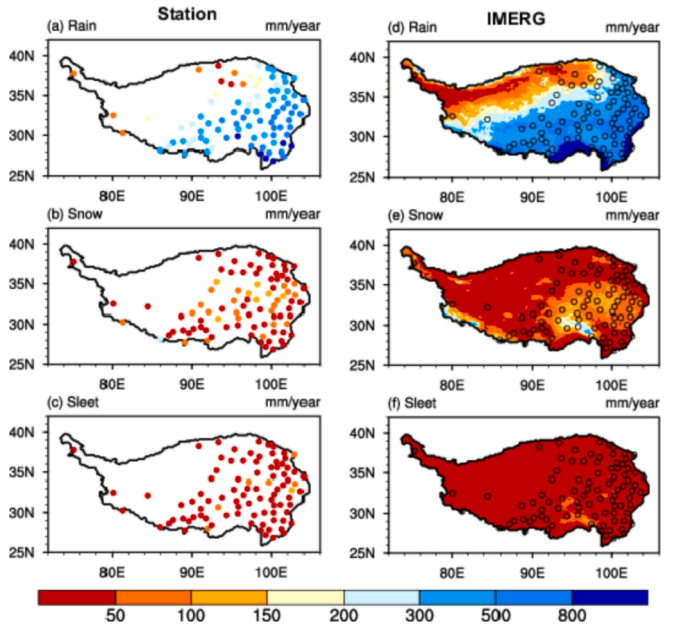

Fig. 2. The spatial distributions of annual total amount of (a) rain, (b) snow and (c) sleet during 2010–2013 in the gauge observation. Subplots (d) to (f) correspond to subplots (a) to (c), but in the IMERG product. The hollow circles in subplots (d) to (f) represent the pixels selected in the IMERG product.

procedures. (1) The weather phenomena are manually recorded before 2014, the full period of the data we collected is 2010–2015, and there are many missing values in 2014 and 2015. Therefore, the period of 2010–2013 is selected first. (2) There are three variables, including present weather, past weather 1 and past weather 2 can provide the weather phenomena information. However, past weather 1 and past weather 2 were often not recorded. Therefore, only present weather is used in this study and the time resolution is every 3 h. (3) 90 stations are selected according to the proportion of effective sample size of weather phenomena data. The missing data is less than 1% every year in these selected stations.

We double-check the accuracy of the weather phenomena data with the daily precipitation data. The precipitation amount (arithmetic mean of the 90 stations) on days recorded as precipitation day in the weather phenomena dataset account for approximately 97% of the total precipitation amount in the daily precipitation dataset provided by CMA in 2010–2013. Therefore, the weather phenomena dataset can reasonably provide the precipitation phase information.

Since the ground-based observation is point measurement of precipitation, we take the approach of comparing the station data with the precipitation in the IMERG product at the points nearest to the stations. Therefore, 90 IMERG pixels are selected. If the values are missing in the station data, the corresponding values in the IMERG pixels will be masked to make the comparison more effectively. In order to simplify the description, the "regional mean" of a variable in a certain region represent the arithmetic mean of this variable in the stations over this region in the evaluation section.

2.3. Distinguish different phases of precipitation over TP

In the station data, the precipitation phase is divided into three phases, rain, sleet, and snow. The three-hourly station data are firstly pre-processed to provide daily values. For precipitation amount, the amounts of precipitation in different phases are summed up for each day. For precipitation days (days when precipitation amount larger than 0.1 mm), if multiple phases of precipitation occur on a certain day, then this day will be divided proportionally according to their frequencies. Take the 90 stations as a whole, the total amount of rain, sleet, and snow account for 88.8%, 3.4%, and 7.8%% of the total precipitation amount, respectively. Rain days, sleet days, and snow days account for 78.6%, 4.4%, and 17.0% of the total precipitation days, respectively.

In the IMERG products, PL is a variable used for distinguishing rain, sleet, and snow, and the value of the probability ranges from 0% to 100%. The larger the probability value is, the more likely the precipitation is rain. Ordinarily, liquid precipitation happens when wet-bulb temperature (Tw) higher than 0 °C and PL is high in this condition. Frozen hydrometeors occur around or below Tw less than 0 °C, PL varies from around 50% to very low. The mixed category is likely to occur around the PL = 50% mark. Although the frequency of sleet is much less than rain and snow, the range of PL for sleet is large.

We try to find a value of PL denoted as PL_{const} to make the proportions of the three precipitation phases provided by the IMERG product consistent with those from ground-based observations, and the specific criteria should match with the followings: if PL is larger than PL_{const}, precipitation is treated as rain; if PL is smaller than 100% minus PL_{const} (100%-PL_{const}), precipitation is treated as snow; otherwise, precipitation is treated as sleet. The total absolute bias is the sum of the absolute biases of the proportions of rain, snow, and sleet. For example, when we choose 80% as PL_{const}, the proportions of the amount of rain, snow, and sleet in the IMERG product are 88.8%, 8.1% and 3.1%, respectively. In the ground stations, the corresponding values are 88.8%, 7.8%, and 3.4%, respectively. Therefore, the total absolute bias is |88.8%-88.8%|+|8.1%-7.8%|+|3.1%-3.4%|=0.6%. |a| represents the absolute value of a.

The total absolute bias of the amount of the three precipitation phases reaches the minimum when PL_{const} is set to 82% (Fig. 1a), while the total absolute bias of the frequency of the three precipitation phases reaches the minimum when the value is set to 77% (Fig. 1b). Combining the two values calculated based on precipitation amount and precipitation days, 80% is determined as the threshold for distinguishing

precipitation phases over the TP. In another word, if the probability of liquid precipitation in a certain half-hour is larger than 80%, precipitation that occurred in this half-hour will be treated as rain; if the probability of liquid precipitation in this half hour is smaller than 20%, precipitation occurred in this half-hour will be treated as snow; otherwise, precipitation occurred in this half-hour will be treated as sleet.

2.4. Estimating skill of IMERG product

The performance of the IMERG product is evaluated using the following metrics (Chen et al., 2013):

$$Skill = \frac{(1+R)^2}{(SDR + \frac{1}{SDR})^2} \quad (1)$$

R is the correlation between the precipitation (rain, snow) in the 90 selected grids in the IMERG product and the corresponding 90 ground stations. SDR is the ratio of the standard deviations of precipitation (rain, snow) in the 90 grids and the corresponding 90 stations. Therefore, both spatial distribution and magnitude are considered in this formula. The skill is higher when the value is closer to 1.0.

2.5. Definition of sub-regions and different intensity levels of rain and snow

In order further evaluate the performance of the IMERG product in estimating precipitation in different phases over the TP, we divide the TP into two parts: the southern Tibetan Plateau (STP) and the northern Tibetan Plateau (NTP), by 32°N according to general climate regimes and the location of ground stations.

We divide rain and snow into four intensity levels: light, moderate, heavy, and storm, respectively, according to the criteria of the CMA in classifying rain and snow intensities. The detailed information is listed in Table 1.

3. Results

3.1. Evaluation of IMERG precipitation product

The precipitation amount in IMERG product over the TP is first evaluated. In the station data, generally, total annual rainfall decreases from the southeast to the northwest of the TP (Fig. 2a), with the values in the large center greater than 800 mm. The total annual snowfall is much less than that of rainfall in almost all the 90 stations over the TP (Fig. 2b) and the averaged snow/rain ratio in the 90 stations is 12%. The eastern part of the central TP is an area with more snowfall, and the values are close to 150 mm in some stations. The spatial distribution of the amount of sleet is similar to that of snow, but the magnitudes are much smaller (Fig. 2c). The IMERG product shows much more spatial distribution characteristics of precipitation in different phases than the station data (Fig. 2d-f). Generally, IMERG performs well in capturing the spatial distributions of rain, snow, and sleet. The precipitation amounts in different phases in IMERG are a little more than those in the station data, but within an acceptable range.

The annual cycle of regional mean precipitation in different phases shows that the peak of rainfall occurs in summer (Fig. 3a). The amount of rain is larger than 100 mm per month in July. The snowfall is mainly concentrated in boreal spring and autumn and the amount of snow is larger than that of rain in boreal winter months. The amount of sleet is small and the peak value occurs in May (Fig. 3a). Although rainfall in the IMERG product is more than that in the station data in July and August, annual cycles of precipitation in different phases are reasonably characterized (Fig. 3b).

Table 1
Definition of different intensity levels of rain and snow.

Level	Rain (mm/day)	Snow (mm/day)
Light	0.1–9.9	0.1–2.4
Moderate	10–24.9	2.5–4.9
Heavy	25–49.9	5–9.9
Storm	≥50	≥10

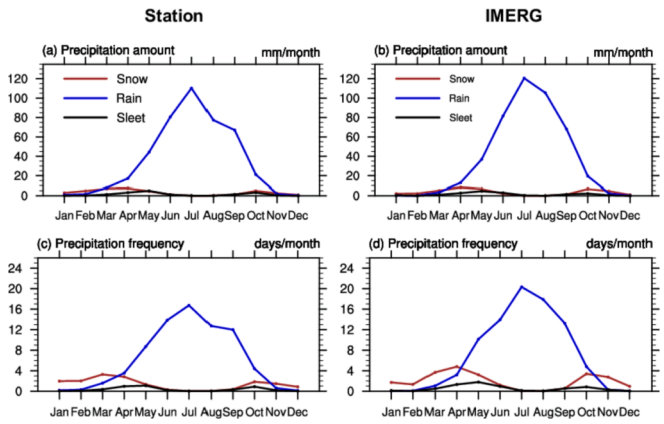

Fig. 3. Monthly mean of (a) amounts, and (c) days of precipitation in different phases during 2010–2013 in the 90 stations. Subplots (b) and (d) correspond to subplots (a) and (c), but in the IMERG product. The values derived from the nearest grids to the stations are used in the IMERG product.

In order to quantitatively evaluate the performance of the IMERG product, we use formula (1) to obtain the skill scores. The skill is higher when the value is closer to 1.0. In general, IMERG shows higher skill in estimating rain than snow (Fig. 5a). The skill scores for the annual amount of precipitation, rain and snow are 0.84, 0.81 and 0.42 respectively. The R and SDR of annual snowfall are 0.3 and 0.92, respectively, which means that the magnitudes of snowfall in the IMERG product and the station observation are comparable but the spatial distributions of snowfall in the 90 grids in IMERG product and the corresponding 90 stations are relatively different. For different seasons, the skill scores for the amount of precipitation and rain are higher in boreal spring, summer and autumn than in winter, and the reason is that winter precipitation is primarily snow in all the 90 stations.

The regional mean bias (mean bias in the stations over a certain region) of precipitation amount is further investigated (Fig. 6a). The regional averaged annual precipitation amount in the IMERG product is comparable with that in the station observation, and the absolute (relative) biases over the NTP and STP are −0.9 mm/month and 5.0 mm/month (-2.8% and 10.2%), respectively. Consistent with Fig. 3, there are wet biases in summer in both of the NTP and STP, and the relative biases of rain in the two regions are comparable (15.5% and 14.1%). Absolute biases of snowfall in winter in the two regions are small (within ± 2 mm/month), but the relative biases are obvious, especially in the NTP (−66%).

The precipitation days (frequency) in the IMERG product are also evaluated. The spatial distributions of the frequency of different precipitation phases are similar to the corresponding spatial distributions of the precipitation amount (Figs. 2 and 4). There are more than 120 rainy days per year in some stations along the southeast of the TP in the station data (Fig. 4a). Snowy days are much less frequent than rainy days throughout the TP and are concentrated in 10 to 40 days for most stations (Fig. 4b). The average snowy/rainy days ratio in the 90 stations is 26%. The IMERG product also performs well in capturing the spatial distributions and magnitudes of the frequency of precipitation in different phases (Fig. 4d–f). Compared with the precipitation amount, the bias of precipitation frequency is larger in the IMERG product (Figs. 2 and 4). One possible reason for this bias is that light precipitation days are more frequent in the satellite observation than in the ground observation.

The peak of rainy days averaged in the 90 stations also occurs in

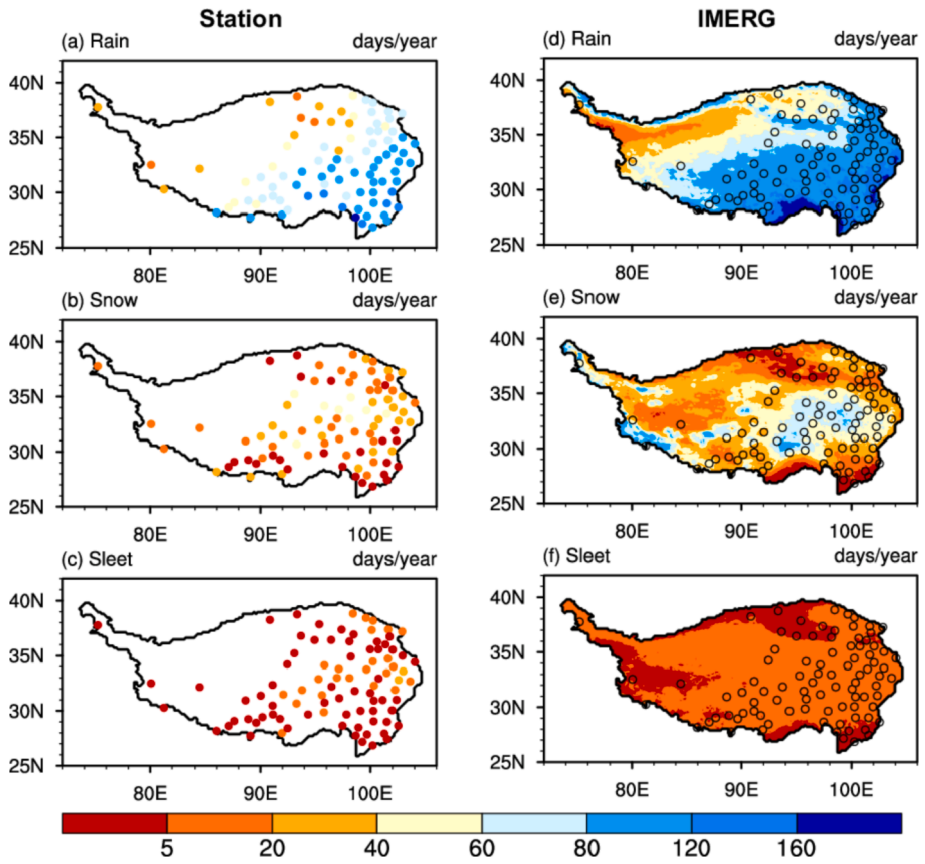

Fig. 4. The spatial distributions of (a) rain, (b) snow, and (c) sleet days per year during 2010–2015 in the station observation. Subplots (d) to (f) correspond to subplots (a) to (c), but in the IMERG product. The hollow circles in subplots (d) to (f) represent the pixels selected in the IMERG product.

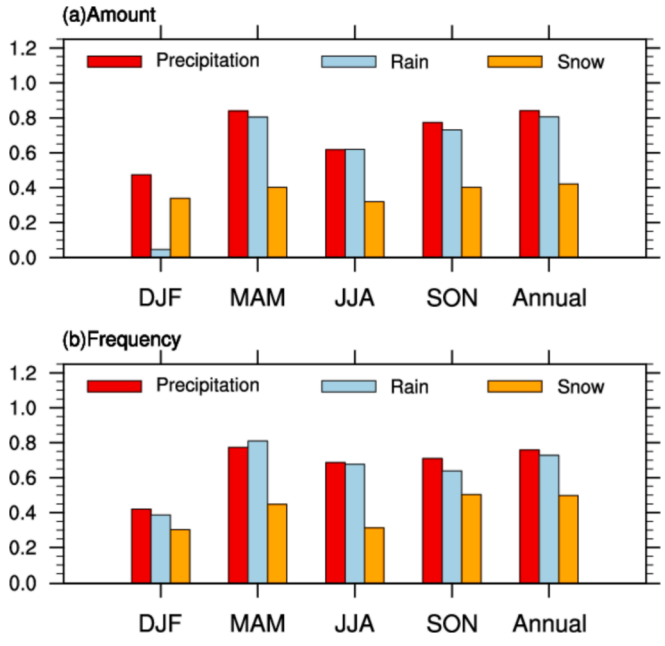

Fig. 5. The skill scores of (a) amount and (b) frequency of precipitation (red bar), rain (light blue bar) and snow (orange bar). Comparing the values in the selected 90 grids in the IMERG product with values in the corresponding 90 ground stations. DJF = boreal winter, MAM = boreal spring, JJA = boreal summer, SON = boreal autumn, Annual = the whole year. (For interpretation of the references to colour in this figure legend, the reader is referred to the web version of this article.)

boreal summer months and there are more than 15 rainy days per month in July (Fig. 3c). The average snowy days in the 90 stations are approximately 3 days in March and April and sleet days are about 1 day in May (Fig. 3c). Consistent with the results above, precipitation in different phases occurs more frequently in the IMERG product than in the station data, but the bias is within an acceptable range and the annual cycle of the precipitation frequency matches well with that in the station data (Fig. 3d).

The IMERG product shows acceptable skill in estimating the frequency of precipitation and its two phases, and the skill scores are comparable with those for the corresponding amount (Fig. 5a and b). The regional averaged annual precipitation frequency in the two subregions are both approximately 20% (Fig. 6b). Compared with precipitation amount, the regional mean biases of precipitation frequency are more uniform across different seasons and regions over the TP. The IMERG product reported more rainy days and snowy days in spring, summer, and autumn in both the NTP and STP than the station observation (Fig. 6b). Conditions for winter are different. The IMERG product reported more snowy days in STP and less snowy days in NTP than the station observation and the relative biases are more than 60% and −60% in the two regions, respectively. It should be noted that the rainy days are negligible in winter and the sample size for the calculation of biases in rainy days in winter is small.

In general, the IMERG product performs well in capturing the climatic characteristics of precipitation in different phases over the TP and shows higher skill in rain estimate than in snow estimate. The main precipitation type in winter is solid in the 90 stations over the TP, and conceivably, the IMERG product performs better in the other three seasons than in winter. The regional mean biases in the NTP and STP are comparable for rain and snow in different seasons. It should be noted that the statistics and results shown above are all derived from the 90

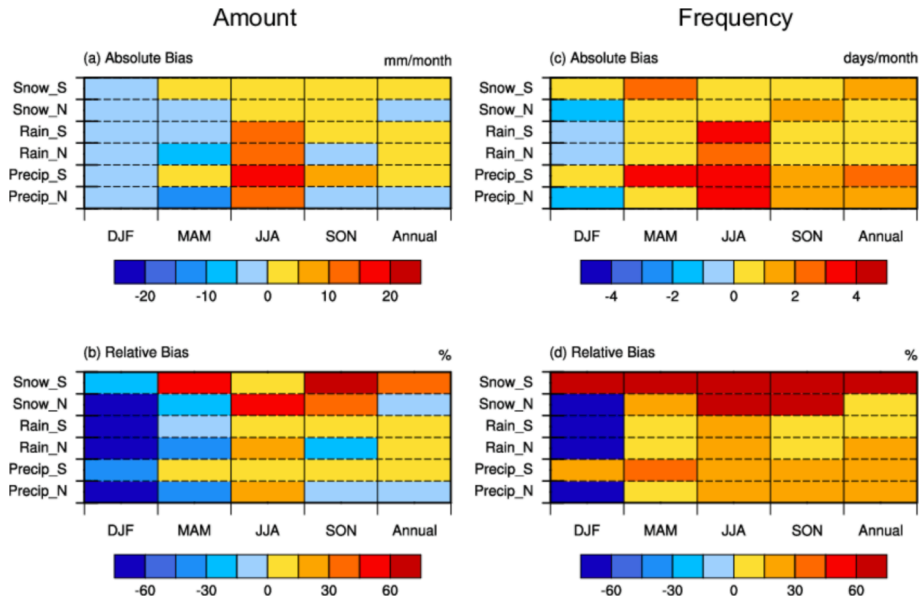

Fig. 6. Averaged (a) absolute and (b) relative bias of amount of precipitation (Precip), rain and snow in stations in northern (N) and southern (S) Tibetan Plateau. Subplots (c) and (d) correspond to subplots (a) and (b), but for frequency.

stations and the corresponding IMERG pixels. The sparsely distributed ground stations (especially in the northwestern TP) and the complex terrain over the TP limits the representativeness of the results, and more ground-based observations are needed to assess the IMERG product more comprehensively in the future research.

Previous studies indicate that the performance of the IMERG product varies in different regions and climate conditions (Chen et al., 2018; Alsumaiti et al., 2020; Pradhan et al., 2022). It shows higher skill in lower latitude regions than in higher latitude regions (Chen and Li, 2016). Additionally, complex terrain may make it more difficult to estimate precipitation (Ma et al., 2018; Navarro et al., 2019; Wang et al., 2019). As mentioned above, the precipitation days are more reported in the IMERG product than in the station observation, and the possible reason is for this is the evaporation of light precipitation in the atmosphere (Wang et al., 2019). Despite that the IMERG product shows better performance in capturing snowfall than other satellite-based precipitation product (Sadeghi et al., 2019), there are still room for improvement. The possible reason is the limitation of passive microwave retrievals and infrared information at cold or snow-covered background surfaces (Yong et al., 2015; Lu and Yong, 2018).

In the next part of this study, we investigate the changes in precipitation in different phases in the last two decades using the IMERG product.

3.2. Changes of precipitation in different phases

The annual precipitation amount has significantly increased in most areas of the TP in the last two decades, with maximal values of over 50 mm per decade occurring in the central part of eastern TP. The precipitation amount has decreased in the last two decades in some parts of southwest TP, but this change is not significant (Fig. 7a). Previous studies indicate that annual precipitation amount has increased in most parts of the TP since the 1960 s (Wang et al., 2018), but the changing pattern may be different during different study periods (Li et al., 2010; Tong et al., 2014b; Zhang et al., 2017). The changing patterns of the amounts of rain, snow, and sleet are similar to that of total precipitation and the changing magnitudes of precipitation are dominated by that of rain, accounting for up to 80% over most parts of the TP (Fig. 7a-d). Considering that precipitation changes may be different among different months. We select two regions to further investigate the changes in the annual cycle of precipitation over the TP. As shown in Fig. 7a, one region

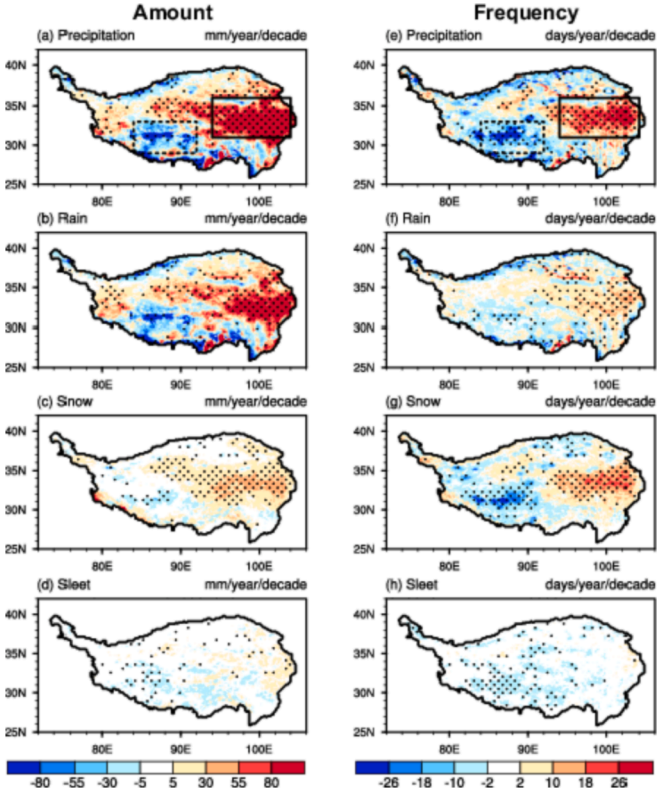

Fig. 7. Trends of precipitation amount (left column) and frequency (right column) in different phases. The dotted areas are statistically significant at the 10% level according to Student's *t*-test. The solid box represents region 1 and dashed box represents region 2.

is in the central part of eastern TP (region 1; solid box) and the other one is in the southwestern TP (region 2; dashed box).

Regional mean linear trends of precipitation amount and frequency in the two selected regions are shown in Figs. 8 and 9. Precipitation amount has increased almost throughout the year in region 1 in the last two decades. Rainfall is the main contributor to the increase in

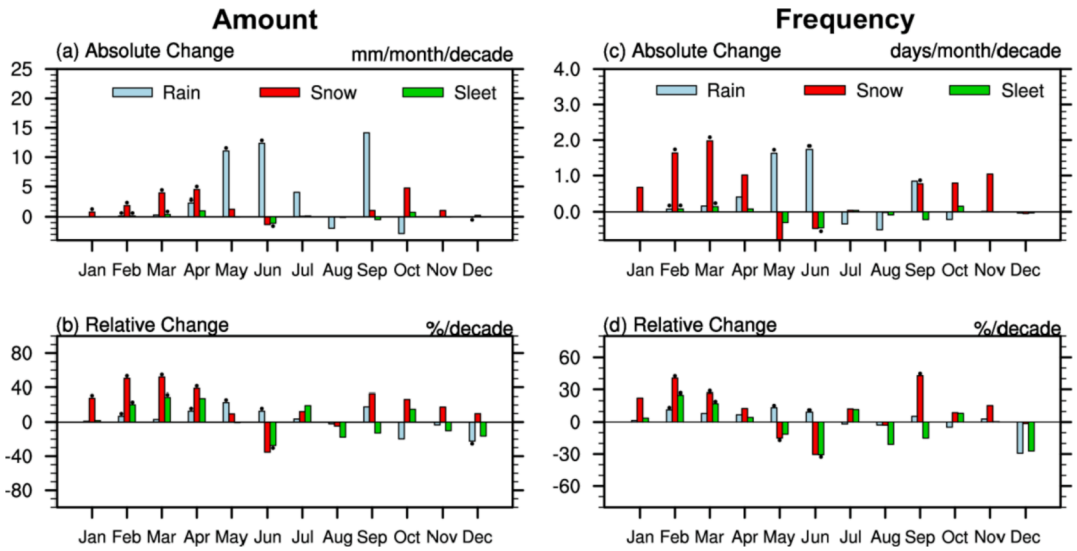

Fig. 8. (a) The trend of the amount of precipitation in different phases averaged over region 1. Subplot (b) is the trend of the amount relative to the climatology during 2001–2020. Subplots (c) and (d) correspond to subplots (a) and (b), but for the frequency of precipitation.

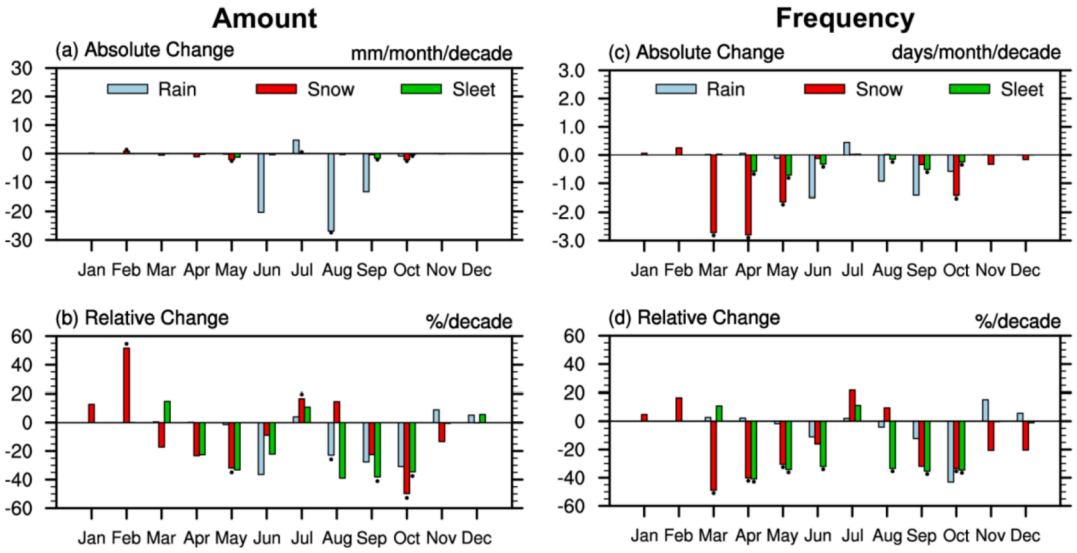

Fig. 9. Corresponds to Fig. 8, but for region 2.

precipitation amount in May to September while the increased precipitation in boreal spring and autumn is mainly contributed by the increase in snowfall (Fig. 8a). The absolute increase in the amount of rain in summer is larger than that of snow in spring and autumn. However, in terms of the relative change (relative to the climatology during 2001–2020), the increase in the amount of snow is larger than that of rain (Fig. 8b). Considering that in climatology, precipitation amount peaks in summer and the regional mean rainfall is much more than snowfall in region 1, the precipitation amount in region 1 has been more dispersed in the past two decades, and the proportion of snowfall has increased.

The overall warming in the past decades is one possible reason for the overall increase of the precipitation amount over the TP, since the water vapor content in the atmosphere increases along with the increase of air temperature, and then, precipitation is expected to increase (Trenberth, 2011) if other conditions remain the same. In addition, the summer precipitation over the TP has experienced an interdecadal transition in the late 1990s, and the increase in precipitation over northern TP is the combined contribution of the positive phase of Atlantic Multi-decadal Oscillation (AMO) and the negative phase of Interdecadal Pacific Oscillation (IPO) (Liu et al., 2021). Besides, the earlier onset of the South Asian summer monsoon may be one important reason for the significant increase of precipitation amount in May in region 1 (Zhang et al., 2017).

As mentioned above, precipitation amount has decreased in the past two decades in region 2, but this decrease is not significant according to Student's *t*-test at the 10% significance level (Fig. 7). Changes in the annual cycle of precipitation in different phases indicate that the decrease in precipitation amount in region 2 is mainly caused by the decrease in rainfall in June and August (Fig. 9a and b). For the mechanism of the precipitation changes in regions 2, Yue et al. (2020) indicate that the monsoon precipitation change over the southern TP shows a decadal variation during 1979–2018 and the mean precipitation over the southern TP decreased from 1998 to 2009 and increased afterward. They also argue that this decadal variation is associated with a large-scale dipolar sea surface temperature pattern between the equatorial central Pacific and the Indo-Pacific warm pool.

The spatial distribution of the trend in the precipitation frequency is

similar to that of the precipitation amount (Fig. 7a and e). Precipitation days have been significantly increased in region 1, with a maximal value of more than 20 days per year per decade. The decrease in precipitation days in region 2 is more evident than that in precipitation amount and the maximal value is also more than −20 days per year per decade (Fig. 7e). The changing patterns of the frequencies of rain, snow, and sleet are also similar to that of precipitation (Fig. 7f–h). but the changing magnitudes of precipitation days are dominated by that of snowy days (Fig. 7e–h), including the increase in region 1 and decrease in region 2.

The absolute increase in precipitation days in region 1 mainly occurs in spring and autumn. The increase in rainy days is concentrated in late spring and early autumn, while the increase in snowy days is concentrated in early spring and late autumn (Fig. 8c). Similarly, the relative increase in the snowy days is larger than that in the rainy days (Fig. 8d). Therefore, precipitation days in region 1 have become more dispersed in the past two decades, and the proportion of snowy days has been increased. Precipitation days have decreased in region 2 almost throughout the year, and this is especially true for snowy days in spring and autumn (Fig. 9c and d).

The results above indicate that both rain and snow have been significantly changed in the past two decades. Precipitation of different intensities may affect the climate and ecosystem differently. In the following part, we divide rain and snow into four levels, light, moderate, heavy, and storm, respectively, according to the criteria of the CMA in classifying rain and snow intensities.

The magnitudes of linear trends in rainfall decrease with the increase of intensity in most parts of the TP and the areas of significant trends are also limited to the central part of eastern TP (Fig. 10a–d). Therefore, the changes in rainfall over the TP in the last two decades are dominated by light and moderate rain. It is worth noting that, from the perspective of regional mean, in region 1 (the area with the largest trend), the light, moderate, heavy, and storm levels account for 32%, 36%, 30%, and 2% of the total rainfall trend, respectively. Similarly, the magnitudes of linear trends of rainy days also decrease with the increase of intensity, and compared with rainfall rate, the changes in rainy days are more concentrated in light rain (Fig. 10e–h). For the regional mean rain-day in region 1, the light, moderate, heavy, and storm levels account for 73%, 20%, 6%, and 1% of the total increase, respectively.

Changes in the snowfall of different intensities all show similar spatial distributions, with larger magnitudes located in the central part of eastern TP (Fig. 11a–d). The light, moderate, heavy, and storm levels account for 40%, 30%, 22%, and 8% of the total regional mean snowfall trend in region 1, respectively. Similar to rainy days, changes in snowy days are dominated by light snow (Fig. 11e–h). In region 1, the light,

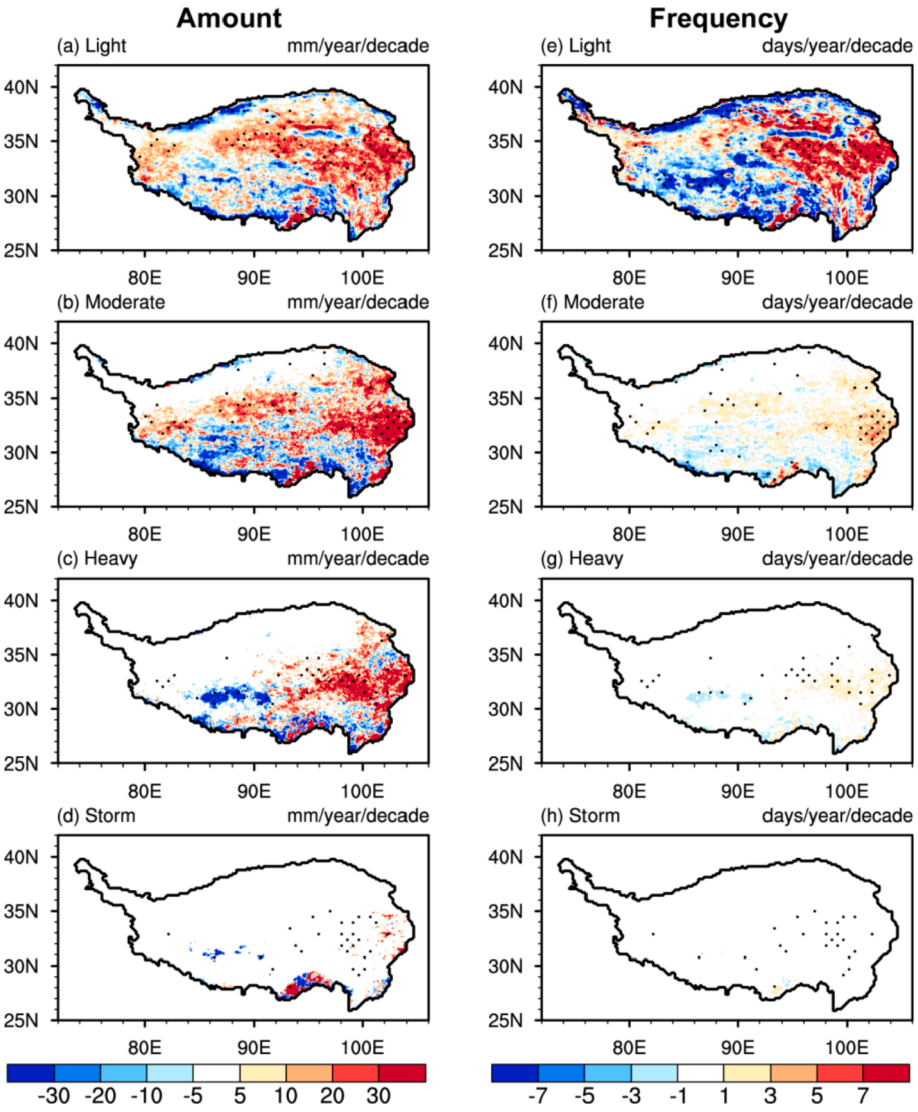

Fig. 10. Trends of rain amount (left column) and frequency (right column) in different levels. The dotted areas are statistically significant at the 10% level according to Student's *t*-test.

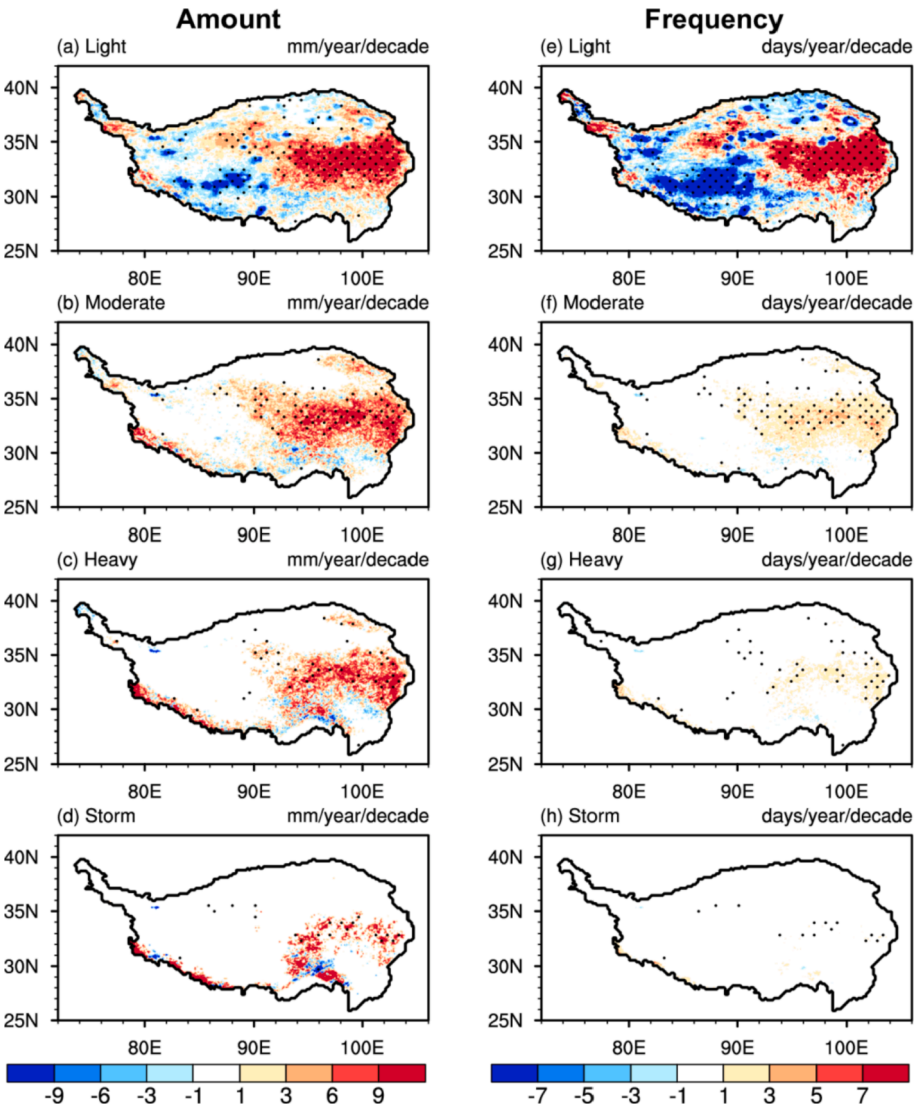

Fig. 11. Corresponds to Fig. 10, but for snow.

moderate, heavy, and storm levels account for 78%, 16%, 5%, and 1% of the total snowy day trend, respectively. In addition, the decrease in precipitation days in region 2 is dominated by the decrease in light snow days (Figs. 9 and 11).

Rain and snow of different intensity levels show similar changing patterns, and the changes in the amount and frequency of rain (snow) are mainly contributed by the changes in light and moderate rain (snow). A previous study also indicates that the precipitation of different intensity levels generally increases in the TP under global warming (Ma et al., 2015).

Changes in the snowy season have an important impact on the climate and water cycle system of the TP and even the whole of East Asia. The snowy days have been increased in region 1 and decreased in region 2. The following part illustrates whether the change in the length of the snowy season is the reason for the changes in the snowy days. Starting from 1st July of each year, the day when the first snow event occurs and the daily precipitation amount greater than 0.1 mm is defined as the beginning of the snowy season. The day when the last snow event occurs and the daily precipitation amount greater than 0.1 mm before the next 1st July is defined as the end of the snowy season.

The beginning, end, and duration of the snowy season over the TP are closely related to local altitude. Areas with higher altitudes often correspond to earlier beginning, later end, and longer duration of the snowy season (Fig. 12a–c). During the past two decades, the start date of the snowy season has been delayed over most parts of the TP, especially in the southwestern TP, with a maximal value of more than 10 days per decade (Fig. 12d). The end date of the snowy season over the TP has been advanced over most parts of the TP, especially in southeastern TP, and the maximal value is also larger than 10 days per decade (Fig. 12e). As a result, the duration of the snowy season over the TP has been getting shorter in the past two decades, especially the southern TP (Fig. 12f). However, it is worth mentioning that changes in the snowy season are not uniform and not significant over most parts of the TP. The above results indicate that the increase in snowy days in most areas of the TP is caused by more frequent snow events in the relatively constant snowy season. The decrease in snowy days in the southwestern TP may be partly caused by the shortening of the snowy season.

4. Summary and conclusion

In this study, the recently updated retrospective IMERG V06 product, calibrated by monthly rain gauge data, is applied to investigate the changing characteristics of precipitation in different phases, especially rain and snow, over the TP during the past two decades. The performance of the IMERG product in capturing the characteristics of rain, snow, and sleet is firstly investigated by comparing it with the ground

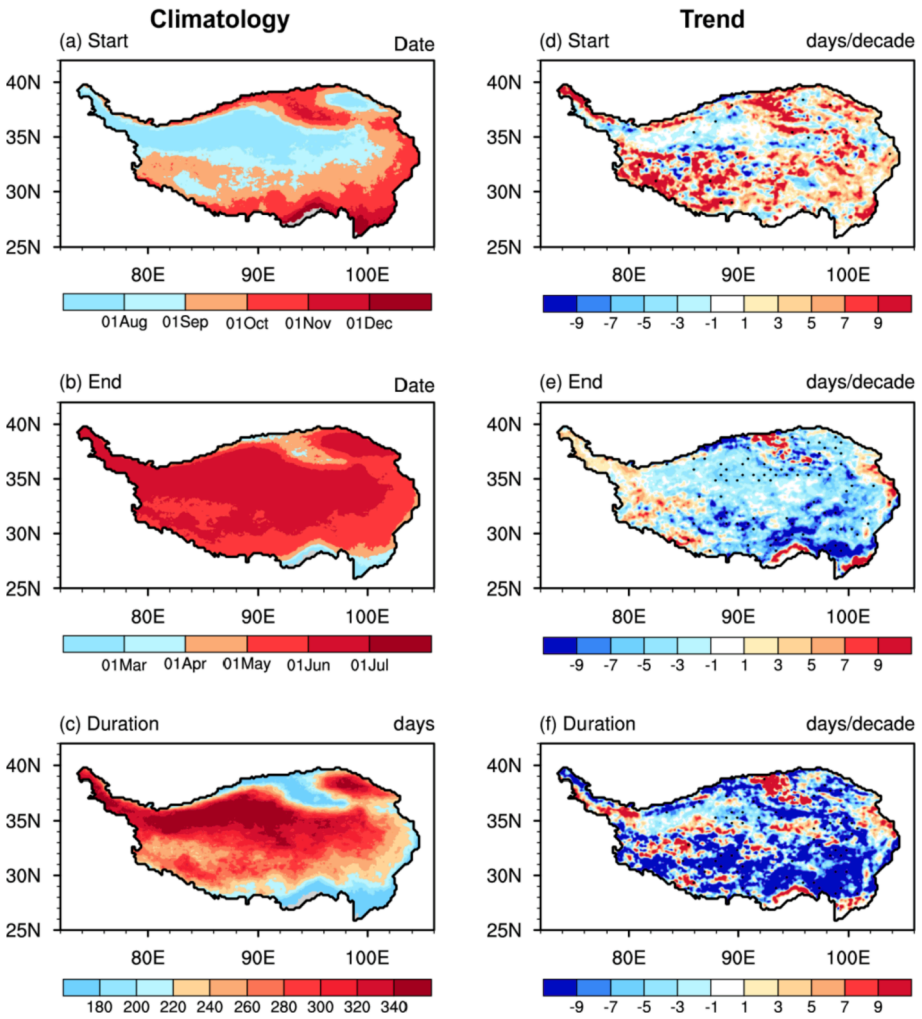

Fig. 12. The (a) start date, (b) end date, and (c) duration of snowy season over the TP during 2001–2020. Subplots (d)-(f) are the trends of the start date, end date, and duration of snowy season during 2001–2020, respectively. The dotted areas in subplots (d)-(f) are statistically significant at the 10% level according to Student's *t*-test.

station data. After confirming that the IMERG product can be used as a reliable source of information to investigate precipitation over the TP, the changes in precipitation in different phases are then investigated. The main conclusions are summarized as follows:

(1) The spatial distributions of precipitation in different phases are similar, decreasing from the southeast to the northwest of the TP. Compared with the station data, the IMERG product exhibits much more spatial features of precipitation over the TP. The IMERG product performs well in capturing the spatial distribution, magnitudes, and annual cycle of the amount and frequency of precipitation in different phases over the TP and the biases are within an acceptable range. The bias of annual precipitation amount (frequency) averaged over the 90 stations is around 10% (20%) in 2010–2013. Furthermore, The IMERG product shows higher skill in estimating rain than snow, and performs better in the other three seasons than in winter. For subregions, the performance of the IMERG product are comparable in the southern and northern parts of the TP.

(2) Both the amount and frequency of the precipitation have increased in the past two decades over most parts of the TP, with maximal values of 50 mm and 20 days per year per decade, respectively, in the central part of eastern TP (region 1). The absolute increase in rainfall is larger than that in snowfall in region 1, but the relative increase is just the opposite. As a result, the precipitation amount in region 1 has been more dispersed in the past two decades.

(3) Changing patterns of amount and frequency of rain, snow, and sleet are similar to those of precipitation. Changes in rainfall are the main contributors to the total changes in the amount of precipitation in the past two decades while changes in snowy days dominate the changes in precipitation days. Rain and snow of different intensity levels show similar changing patterns. In addition, increases in light and moderate rain (snow) are the main contributors to the regional mean increases of the amount (about 70%) and frequency (more than 90%) of rain (snow) in region 1.

(4) The snowy season has been shortened over most parts of the TP but this change is not uniform nor significant in most regions. This indicates that the increase in snowy days in most areas of the TP is caused by more frequent snow events in the relatively constant snowy season.

The results in this study indicate that rain and snow have increased in most regions over the TP in the past two decades, and this change is the continuation of the long-term change in the past several decades according to the previous studies (Wang et al., 2018; Zhang et al., 2017). Both global warming and large-scale circulations are contributed to the changes of precipitation over the TP, and these contributions show obvious spatial and seasonal features. The strengthened South Asia

Summer Monsoon, the increased moisture transport from the Indian ocean, the decadal transition of AMO and IPO, and the large-scale sea surface temperature anomaly may have affected the precipitation over the TP (Zhang et al., 2017; Li et al., 2019; Zhang et al., 2019; Yue et al., 2020; Liu et al., 2021).

Previous studies mainly focus on precipitation (rain, snow and sleet) changes, not changes in rain or snow separately. However, causes behind changes in rain and snow may be different. Thus, the different mechanisms for rain and snow at different intensity levels needs to be studied further in the future.

CRediT authorship contribution statement

Donghuan Li: Data curation, Invastigation, Formal analysis, Writing - original draft. **Youcun Qi:** Formal analysis, Writing - review & editing. **Deliang Chen:** Formal analysis, Writing - review & editing.

Declaration of Competing Interest

The authors declare that they have no known competing financial interests or personal relationships that could have appeared to influence the work reported in this paper.

Acknowledgments

Major funding for this research was provided under Strategic Priority Research Program of Chinese Academy of Sciences (XDA2006040101), National Key Research project: “The Tibetan Plateau Land-Air Coupling System Change and Its Global Climate Effect” (No. 91637211), and Hundred Talent Program.

References

Alsumaiti, T.S., Hussein, K., Ghebreyesus, D.T., Sharif, H.O., 2020. Performance of the CMORPH and GPM IMERG Products over the United Arab Emirates. Remote Sens. 12 (9), 1426.

Auer Jr, A.H. (1974). The rain versus snow threshold temperatures. Weatherwise, 27(2), 67-67. 10.1080/00431672.1974.9931684.

Bai, L., Shi, C., Shi, Q., Li, L., Wu, J., Yang, Y., Sun, S., Zhang, F., Meng, J., 2019. Change in the spatiotemporal pattern of snowfall during the cold season under climate change in a snow-dominated region of China. Int. J. Climatol. 39 (15), 5702–5719. https://doi.org/10.1002/joc.6182.

Barnett, T.P., Adam, J.C., Lettenmaier, D.P., 2005. Potential impacts of a warming climate on water availability in snow-dominated regions. Nature 438 (7066), 303–309.

Chen, C., Chen, Q., Duan, Z., Zhang, J., Mo, K., Li, Z., Tang, G., 2018. Multiscale comparative evaluation of the GPM IMERG v5 and TRMM 3B42 v7 precipitation products from 2015 to 2017 over a climate transition area of China. Remote Sensing 10 (6), 944.

Chen, D., Tian, Y., Yao, T., Ou, T., 2016. Satellite measurements reveal strong anisotropy in spatial coherence of climate variations over the Tibet Plateau. Sci. Rep. 6 (1), 1–9.

Chen, F., Li, X., 2016. Evaluation of IMERG and TRMM 3B43 monthly precipitation products over mainland China. Remote Sensing 8 (6), 472.

Chen, L., Yu, Y., Sun, D.Z., 2013. Cloud and water vapor feedbacks to the El Niño warming: are they still biased in CMIP5 models? J. Clim. 26 (14), 4947–4961. https://doi.org/10.1175/JCLI-D-12-00575.1.

Clark, M.P., Slater, A.G., Barrett, A.P., Hay, L.E., McCabe, G.J., Rajagopalan, B., Leavesley, G.H., 2006. Assimilation of snow covered area information into hydrologic and land-surface models. Adv. Water Resour. 29 (8), 1209–1221. https://doi.org/10.1016/j.advwatres.2005.10.001.

Dai, A., 2008. Temperature and pressure dependence of the rain-snow phase transition over land and ocean. Geophys. Res. Lett. 35 (12).

Deng, H., Pepin, N.C., Chen, Y., 2017. Changes of snowfall under warming in the Tibetan Plateau. J. Geophys. Res.: Atmos. 122 (14), 7323–7341.

Ding, B., Yang, K., Qin, J., Wang, L., Chen, Y., He, X., 2014. The dependence of precipitation types on surface elevation and meteorological conditions and its parameterization. J. Hydrol. 513, 154–163.

Duan, A.M., Wu, G.X., 2005. Role of the Tibetan Plateau thermal forcing in the summer climate patterns over subtropical Asia. Clim. Dyn. 24 (7-8), 793–807.

Gao, Y., Cuo, L., Zhang, Y., 2014. Changes in moisture flux over the Tibetan Plateau during 1979–2011 and possible mechanisms. J. Clim. 27 (5), 1876–1893.

Hou, A.Y., Kakar, R.K., Neeck, S., Azarbarzin, A.A., Kummerow, C.D., Kojima, M., Oki, R., Nakamura, K., Iguchi, T., 2014. The global precipitation measurement mission. Bull. Am. Meteorol. Soc. 95 (5), 701–722. https://doi.org/10.1175/BAMS-D-13-00164.1.

Huang, X., Deng, J., Wang, W., Feng, Q., Liang, T., 2017. Impact of climate and elevation on snow cover using integrated remote sensing snow products in Tibetan Plateau. Remote Sens. Environ. 190, 274–288.

Huffman, G.J., Bolvin, D.T., Nelkin, E.J., Wolff, D.B., Adler, R.F., Gu, G., Hong, Y., Bowman, K.P., Stocker, E.F., 2007. The TRMM Multisatellite Precipitation Analysis (TMPA): Quasi-global, multiyear, combined-sensor precipitation estimates at fine scales. J. Hydrometeorol. 8 (1), 38–55.

Huffman, G.J., Stocker, E.F., Bolvin, D.T., Nelkin, E.J., Jackson Tan (2019), GPM IMERG Final Precipitation L3 Half Hourly 0.1 degree x 0.1 degree V06, Greenbelt, MD, Goddard Earth Sciences Data and Information Services Center (GES DISC), [Accessed 25 March 2021]10.5067/GPM/IMERG/3B-HH/06.

Immerzeel, W.W., Van Beek, L.P., Bierkens, M.F., 2010. Climate change will affect the Asian water towers. Science 328 (5984), 1382–1385.

Immerzeel, W.W., Bierkens, M.F.P., 2012. Asia’s water balance. Nat. Geosci. 5 (12), 841–842.

IPCC. Climate Change 2013: The Physical Science Basis[M]. Cambridge, UK, and New York, USA: Cambridge University Press, 2013.

Islam, M.A., Yu, B., Cartwright, N., 2020. Assessment and comparison of five satellite precipitation products in Australia. J. Hydrol. 590, 125474. https://doi.org/10.1016/j.jhydrol.2020.125474.

Jiang, L., Bauer-Gottwein, P., 2019. How do GPM IMERG precipitation estimates perform as hydrological model forcing? Evaluation for 300 catchments across Mainland China. J. Hydrol. 572, 486–500.

Joyce, R.J., Janowiak, J.E., Arkin, P.A., Xie, P., 2004. CMORPH: A method that produces global precipitation estimates from passive microwave and infrared data at high spatial and temporal resolution. J. Hydrometeorol. 5 (3), 487–503.

Kang, S., Xu, Y., You, Q., Flügel, W.-A., Pepin, N., Yao, T., 2010. Review of climate and cryospheric change in the Tibetan Plateau. Environ. Res. Lett. 5 (1), 015101. https://doi.org/10.1088/1748-9326/5/1/015101.

Kuang, X., Jiao, J.J., 2016. Review on climate change on the Tibetan Plateau during the last half century. J. Geophys. Res.: Atmos. 121 (8), 3979–4007. https://doi.org/10.1002/2015JD024728.

Kubota, T., Shige, S., Hashizume, H., Aonashi, K., Takahashi, N., Seto, S., Hirose, M., Takayabu, Y.N., Ushio, T., Nakagawa, K., Iwanami, K., Kachi, M., Okamoto, K., 2007. Global precipitation map using satellite-borne microwave radiometers by the GSMaP project: Production and validation. IEEE Trans. Geosci. Remote Sens. 45 (7), 2259–2275.

Kummerow, C., Barnes, W., Kozu, T., Shiue, J., Simpson, J., 1998. The tropical rainfall measuring mission (TRMM) sensor package. J. Atmos. Oceanic Technol. 15 (3), 809–817.

Li, Y., Su, F., Chen, D., Tang, Q., 2019. Atmospheric water transport to the endorheic Tibetan plateau and its effect on the hydrological status in the region. J. Geophys. Res.: Atmos. 124 (23), 12864–12881.

Li, Y., Cao, L., Gao, S., Luo, B., 2010. The current stage and development of MICAPS. Meteorol. Monthly 36 (7), 50–55. In Chinese with an English abstract.

Liu, Y., Chen, H., Li, H., Zhang, G., Wang, H., 2021. What induces the interdecadal shift of the dipole patterns of summer precipitation trends over the Tibetan Plateau? Int. J. Climatol. 41 (11), 5159–5177.

Loth, B., Graf, H.F., Oberhuber, J.M., 1993. Snow cover model for global climate simulations. J. Geophys. Res.: Atmos. 98 (D6), 10451–10464.

Lu, D., Yong, B., 2018. Evaluation and hydrological utility of the latest GPM IMERG V5 and GSMaP V7 precipitation products over the Tibetan Plateau. Remote Sensing 10 (12), 2022.

Ma, S., Zhou, T., Dai, A., Han, Z., 2015. Observed changes in the distributions of daily precipitation frequency and amount over China from 1960 to 2013. J. Clim. 28 (17), 6960–6978. https://doi.org/10.1175/JCLI-D-15-0011.1.

Ma, Y., Yang, Y., Han, Z., Tang, G., Maguire, L., Chu, Z., Hong, Y., 2018. Comprehensive evaluation of ensemble multi-satellite precipitation dataset using the dynamic bayesian model averaging scheme over the Tibetan Plateau. J. Hydrol. 556, 634–644.

Marks, D., Dozier, J., 1992. Climate and energy exchange at the snow surface in the alpine region of the Sierra Nevada: 2. Snow cover energy balance. Water Resour. Res. 28 (11), 3043–3054. https://doi.org/10.1029/92WR01483.

Moazami, S., Najafi, M.R., 2021. A comprehensive evaluation of GPM-IMERG V06 and MRMS with hourly ground-based precipitation observations across Canada. J. Hydrol. 594, 125929. https://doi.org/10.1016/j.jhydrol.2020.125929.

Navarro, A., García-Ortega, E., Merino, A., Sánchez, J.L., Kummerow, C., Tapiador, F.J., 2019. Assessment of IMERG precipitation estimates over Europe. Remote Sensing 11 (21), 2470.

Pradhan, R.K., Markonis, Y., Vargas Godoy, M.R., Villalba-Pradas, A., Andreadis, K.M., Nikolopoulos, E.I., Papalexiou, S.M., Rahim, A., Tapiador, F.J., Hanel, M., 2022. Review of GPM IMERG performance: a global perspective. Remote Sens. Environ. 268, 112754. https://doi.org/10.1016/j.rse.2021.112754.

Ren, Z., Zhang, Z., Sun, C., Liu, Y., Li, J., Ju, X., Wang, H., 2015. Development of three-step quality control system of real-time observation data from AWS in China. Meteorol. Mon 41, 1268–1277. https://doi.org/10.7519/j.issn.1000-0526.2015.10.010.

Sadeghi, L., Saghafian, B., Moazami, S., 2019. Evaluation of IMERG and MRMS remotely sensed snowfall products. Int. J. Remote Sens. 40 (11), 4175–4192.

Sims, E.M., Liu, G., 2015. A parameterization of the probability of snow–rain transition. J. Hydrometeorol. 16 (4), 1466–1477.

Slater, A.G., Schlosser, C.A., Desborough, C.E., Pitman, A.J., Henderson-Sellers, A., Robock, A., Vinnikov, K.Y., Entin, J., Mitchell, K., Chen, F., Boone, A., Etchevers, P., Habets, F., Noilhan, J., Braden, H., Cox, P.M., de Rosnay, P., Dickinson, R.E., Yang, Z.-L., Dai, Y.-J., Zeng, Q., Duan, Q., Koren, V., Schaake, S., Gedney, N., Gusev, Y.M., Nasonova, O.N., Kim, J., Kowalczyk, E.A., Shmakin, A.B., Smirnova, T.

G., Verseghy, D., Wetzel, P., Xue, Y., 2001. The representation of snow in land surface schemes: Results from PILPS 2 (d). J. Hydrometeorol. 2 (1), 7–25.
Tang, G., Clark, M.P., Papalexiou, S.M., Ma, Z., Hong, Y., 2020. Have satellite precipitation products improved over last two decades? A comprehensive comparison of GPM IMERG with nine satellite and reanalysis datasets. Remote Sens. Environ. 240, 111697. https://doi.org/10.1016/j.rse.2020.111697.
Tong, K., Su, F., Yang, D., Hao, Z., 2014a. Evaluation of satellite precipitation retrievals and their potential utilities in hydrologic modeling over the Tibetan Plateau. J. Hydrol. 519, 423–437.
Tong, K., Su, F., Yang, D., Zhang, L., Hao, Z., 2014b. Tibetan Plateau precipitation as depicted by gauge observations, reanalyses and satellite retrievals. Int. J. Climatol. 34 (2), 265–285. https://doi.org/10.1002/joc.3682.
Trenberth, K.E., 2011. Changes in precipitation with climate change. Clim. Res. 47 (1), 123–138.
Wang, J., Zhang, M., Wang, S., Ren, Z., Che, Y., Qiang, F., Qu, D., 2016. Decrease in snowfall/rainfall ratio in the Tibetan Plateau from 1961 to 2013. J. Geog. Sci. 26 (9), 1277–1288.
Wang, X., Pang, G., Yang, M., 2018. Precipitation over the Tibetan Plateau during recent decades: a review based on observations and simulations. Int. J. Climatol. 38 (3), 1116–1131.
Wang, S., Liu, J., Wang, J., Qiao, X., Zhang, J., 2019. Evaluation of GPM IMERG V05B and TRMM 3B42V7 Precipitation products over high mountainous tributaries in Lhasa with dense rain gauges. Remote Sensing 11 (18), 2080.
Wu, G., Liu, Y., He, B., Bao, Q., Duan, A., Jin, F.F., 2012. Thermal controls on the Asian summer monsoon. Sci. Rep. 2 (1), 1–7.
Wu, S., Yin, Y., Zheng, D., Yang, Q., 2007. Climatic trends over the Tibetan Plateau during 1971–2000. J. Geog. Sci. 17 (2), 141–151.
Xu, X., Lu, C., Shi, X., Gao, S., 2008. World water tower: an atmospheric perspective. Geophys. Res. Lett. 35 (20) https://doi.org/10.1029/2008GL035867.
Xu, Z.X., Gong, T.L., Li, J.Y., 2007. Decadal trend of climate in the Tibetan Plateau—regional temperature and precipitation. Hydrol. Process. https://doi.org/10.1002/hyp.6.
Yang, K., Wu, H., Qin, J., Lin, C., Tang, W., Chen, Y., 2014. Recent climate changes over the Tibetan Plateau and their impacts on energy and water cycle: a review. Global Planet. Change 112, 79–91.
Yao, T., Thompson, L., Yang, W., Yu, W., Gao, Y., Guo, X., Yang, X., Duan, K., Zhao, H., Xu, B., Pu, J., Lu, A., Xiang, Y., Kattel, D.B., Joswiak, D., 2012. Different glacier status with atmospheric circulations in Tibetan Plateau and surroundings. Nat. Clim. Change 2 (9), 663–667.
Yao, T., Pu, J., Lu, A., Wang, Y., Yu, W., 2007. Recent glacial retreat and its impact on hydrological processes on the Tibetan Plateau, China, and surrounding regions. Arct. Antarct. Alp. Res. 39 (4), 642–650.
Yong, B., Liu, D., Gourley, J.J., Tian, Y., Huffman, G.J., Ren, L., Hong, Y., 2015. Global view of real-time TRMM multisatellite precipitation analysis: Implications for its successor global precipitation measurement mission. Bull. Am. Meteorol. Soc. 96 (2), 283–296.
You, Q., Min, J., Zhang, W., Pepin, N., Kang, S., 2015. Comparison of multiple datasets with gridded precipitation observations over the Tibetan Plateau. Clim. Dyn. 45 (3-4), 791–806.
You, Q., Fraedrich, K., Ren, G., Ye, B., Meng, X., Kang, S., 2012. Inconsistencies of precipitation in the eastern and central Tibetan Plateau between surface adjusted data and reanalysis. Theor. Appl. Climatol. 109 (3), 485–496. https://doi.org/10.1007/s00704-012-0594-1.
Yuan, S., Zhu, L., Quiring, S.M., 2021. Comparison of two multisatellite algorithms for estimation of tropical cyclone precipitation in the United States and Mexico: TMPA and IMERG. J. Hydrometeorol. 22 (4), 923–939.
Yue, S., Wang, B., Yang, K., Xie, Z., Lu, H., He, J., 2020. Mechanisms of the decadal variability of monsoon rainfall in the southern Tibetan Plateau. Environ. Res. Lett. 16 (1), 014011. https://doi.org/10.1088/1748-9326/abcb36.
Zhang, C., Tang, Q., Chen, D., Van Der Ent, R.J., Liu, X., Li, W., Haile, G.G., 2019. Moisture source changes contributed to different precipitation changes over the northern and southern Tibetan Plateau. J. Hydrometeorol. 20 (2), 217–229. https://doi.org/10.1175/jhm-d-18-0094.1.
Zhang, W., Zhou, T., Zhang, L., 2017. Wetting and greening Tibetan Plateau in early summer in recent decades. J. Geogr. Res.: Atmos. 122 https://doi.org/10.1002/2017JD026468.